The Effects of Thin-Walled Structure on Vehicle Occupants' Safety and Vehicle Crashworthiness

Ali Balaei Sahzabi[1], Mohsen Esfahanian[1]

[1]Department of Mechanical Engineering, Isfahan University of Technology, Isfahan, Iran, 84156

Abstract

This article investigates the effects of using a thin-walled structure in the chassis front rails in the automotive industry. In frontal accidents, the front rails of the vehicle chassis, increases vehicle crash-worthiness and occupants' safety by plastic deformation, energy absorption, increasing the crash duration and reducing the load and injuries to the occupants. The objective is to optimize the thin-walled structure of the bumper and the direct beams in the front chassis rails. An explicit FEM full vehicle model with a dummy, safety belts, and air bags are used for the modeling and analysis of the applied loads on the vehicle and the occupants. The FMVSS No. 208 and ECE No. 94 standards are considered for the simulation of a vehicle accident. Finally, the proper model will be selected based on the results.

Keywords: *Crashworthiness, Chassis front rails, Thin-walled structure, Energy absorption, Head injury criteria, Crash time*

1. Introduction

Thin-walled structures have been used in many industries, such as automotive, to absorb energy. The chassis front rail of the vehicle must have the maximum energy absorption and plastic deformation to minimize load and energy transfer to the occupants and increase crash-worthiness and occupants safety. Therefore, thin-walled structures or thin-walled energy absorbents are used in the chassis front rail. The chassis front rail includes a curved beam, a direct beam, and a bumper beam. Many studies have been conducted about optimization of the thin-walled structure in regard to required objectives.

Mohamed Sheriff et al. [1] studied the effect of using a circular cross section-variable radius structure for two heads of the front beams and beam height on energy absorption. They showed that using the larger radius in anchor side relative to the radius of the loaded side of the beam increases energy absorption of plastic deformation. Zhang and Saigal [2] studied the use of square cross sections in a thin-walled structure by internal auto ancillaries to increase energy absorption. They showed that using internal ancillaries increase energy absorption of plastic deformation. Oliveira et al. [3] studied, both numerically and experimentally, the effect of using curved aluminum alloy thin-walled structures with different thicknesses on more energy absorption and lowering the weight. They showed that using higher thickness increases energy absorption of plastic deformation. Tang et al. [4] studied the effect of using multilayer circular cross sections enforced by internal ancillaries using LS DYNA software. They showed that the suggested structures increase the energy absorption of plastic deforming despite the difficulty and higher cost of construction. Yang and Qi [5] investigated the effect of using filled and hollow square sections under both axial and angular loads to increase specific energy and reduce peak impact force. The considered parameters were thickness and material of thin-walled structures and filler density. They showed that using foam increases energy absorption of plastic deformation and reduces peak impact force. Also, angular loading causes overall deformation toward bending and reduces beam crippling. Tarlochan et al. [6] studied different foaming levels under axial and angular loads to increase specific energy and reduce peak impact force. They showed that using foam under axial loading has more energy consumption of plastic deforming and less peak impact force than under angular load. Zhang et al. [7, 8] studied the buckling for loaded square and circular cross sections. They showed that using internal ancillaries change collapse location and structure buckling. Cho et al. [9] used a notched beam to study energy absorption and plastic deformation. They showed that using notches tends the structure deformation toward crippling and reduces overall bending of the beam. Gupta and Gupta [10] used sections with annealed aluminum and steel with different dimensions in their study. They showed that drilled holes along beam with different

diameters change the number and mode of collapses and prevent overall bending. Ohkami et al. [11], Nishijaki et al. [12] investigated the effect of using a curved beam with various sections and different materials under dynamic and static loading both experimentally and numerically. They examined deformation and collapse of the structure. Thou et al. [13] examined the effect of using two different materials in curve and direct sectors of beams. They showed that using materials with less resistance in a direct section of the beam reduces the overall bending deformation. Tanlak and Sonmez [14] examined various sections with various thicknesses. They modeled automotive as mass-spring-dumper to simulate the boundary conditions of the thin-walled structure. The chassis front rails include curved beams, direct beams, and bumper beams. Direct and bumper beams must have the maximum energy absorption in front side accident, and curved beams must have the minimum deformation. The chassis front rails of the vehicle under study is shown in Fig. 1. The front chassis rail is permitted for deformation in front side accidents, but the passenger cabinet safety requires having the minimum deformation in accidents In most studies, the chassis front rail is modeled as a cantilever beam, load on the other side [1-13]. Therefore, the boundary conditions are assumed in connection of this beam and the chassis of the vehicle. The performance indicators of these simulations are deformation, specific energy absorption, and impact force.

To have a more exact investigation and results, the total vehicle model, dummy, and three beams of the chassis front rails is modeled in this study. In order to examine the results of the thin-walled structure in vehicle accidents and its effect on vehicle safety, the required performance indicators would be vehicle crash time, specific energy absorption, imposed injuries on occupants, and resulted in plastic deformation by the crash.

In this article, five suggested models for thin-walled structures of chassis front rails of the vehicle are investigated. The first model uses a thin-walled structure for direct beam without bumper beam, and the remaining models included the optimized models to be used in direct and bumper beams. The FMVSS No. 208 standard consists of a test with velocities of 15.55 m/s, with a rigid barrier having a complete overlap, are being used to study the safety for these five suggested models in front side accident.

Finally, by investigating results of the suggested models, an appropriate model for chassis front rails of the vehicle is selected. After selection of the appropriate model, simulations of crash tests for FMVSS No. 208 and ECE No. 94 standards are performed to study vehicle safety.

The objective of the optimization of the thin-walled structure in the chassis front rails of the vehicle is increasing the crash-worthiness, the safety of occupants, and the energy absorption in the chassis front rails of the vehicle. Another factor that must be studied is the vehicle's crash time since the imposed loads on occupants are related to the crash time and the imposed acceleration on them.

It is noteworthy that none of the earlier studies considered vehicle crash time and only imposed loads on the occupants because they did not use a full vehicle model.

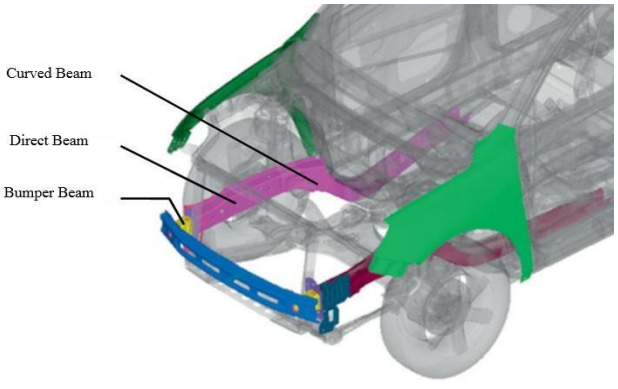

Fig. 1. The parts of chassis front rail.

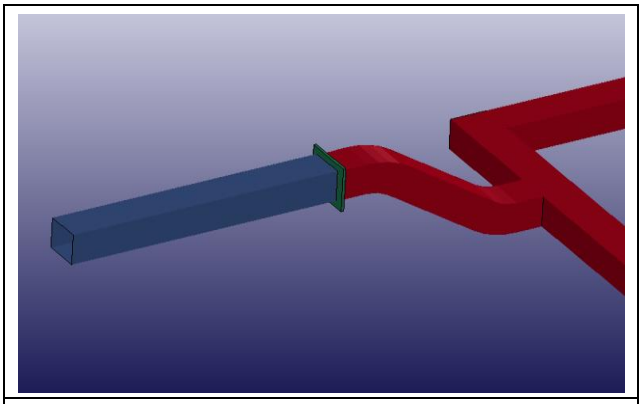

Fig. 2. Modelling the first model.

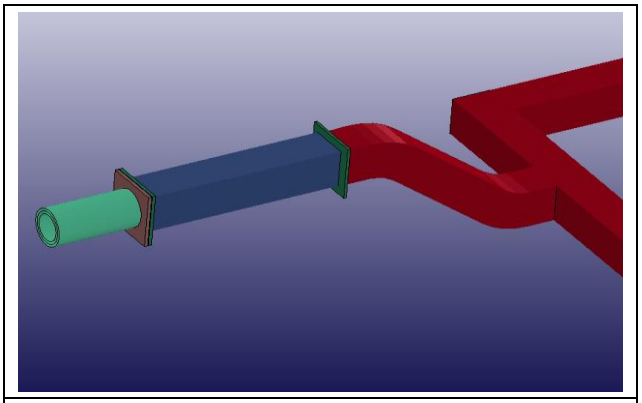

Fig. 3. Modelling of the second model.

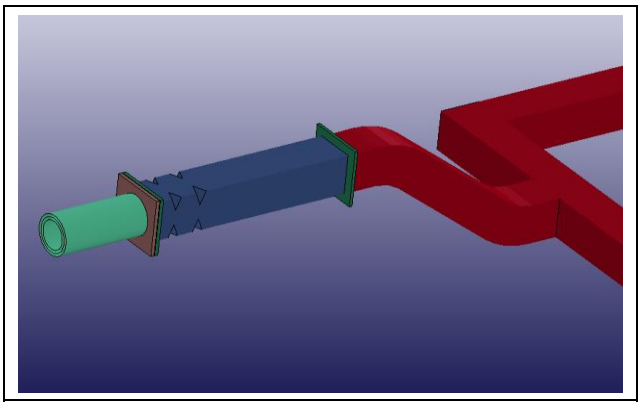

Fig. 4. Modelling the fourth model.

2. Designed models

In this article, five models are suggested for investigating the effect of a thin-walled structure in energy absorption during front side accidents. In all five models, curved beam needs to be harder than the direct beam and the bumper beams, because it has the shortest distance to the cabin. Also, its deformation is in the form of an overall bending which pushes the vehicle's frontal components to the cabin and therefore causing injuries to the passengers. For more hardness and prevention from overall bending, the curved beam is made of a 3 mm St52 steel which is more than the thickness of the direct beam and the bumper beams. Direct beam and bumper beam should

collapse earlier than the curved beam. The direct beam is made of 2 mm thick and St52 steel.

First Model

The thin-walled structure for direct beam without bumper beam was selected for the first model. Cross section of the direct beam is a square with 75 mm side and 0.5 m length. The lower thickness of direct beam with respect to the curved beam is for more plastic deformation and crippling. The first model is shown in Fig. 2.

Second Model

For the second model, a bumper beam with lower strength is added in order to have a smaller amount of bending in the front rails of the chassis and a greater amount of plastic deformation in the direct beams. This concept prevents the damage to the main chassis, in low-speed accidents, and only the bumper beam gets damaged. In high-speed accidents With the addition of a shorter direct beam, forces cause shorter beams to cripple and prevent overall bending of the direct beam. In general, it is more suitable for the direct beam and the bumper beam to not have the overall bending but rather have energy absorption and plastic deformation.

The bumper beam is designed by taking advantage of Dass Goel's study. Dass Goel [15] studied square and circular cross sections in single-layer, two-layer, and three-layer with and without foam. In his study, a thin-walled structure was loaded as a cantilever beam from one side and loaded by a solid surface from another. Dass Goel showed that three-layer circular sections without foam have the maximum energy absorption. Thus, a three-layer circular section without foam is used to design the bumper beam.

The length of the bumper beam is 0.15 m maximum, due to the limitations and in order to have a maximum plastic deformation. The diameters of the three circles are 75, 65, and 55 mm with a thickness of 2 mm. To have a better energy and loads transfer, the diameter of the outer circle is the same as the side of the direct beam which is 75 mm. A bumper beam with Al6063 aluminum alloy material was used to have better energy absorption and have greater plastic deformation. The direct beam was designed like the first model but with 0.35 m shorter. The second model is shown in Fig. 3.

Third Model

The third model is similar to the second model except for selecting a bumper beam with 1 mm in thickness.

Fourth Model

Alavi Nia et al. [16] studied energy absorption and plastic deformation of a square section beam under the axial and angular loads with using symmetrical and asymmetrical notches in four corners of the beam, both by software simulation and experimentally. They showed that using symmetrical notches in four corners of a square cross section can prevent it from overall bending and causes crippling in axial length of the beam. In addition, results showed that the number and location of the notches didn't have a significant effect on energy absorption and notches are mostly effective in deformation and collapse of a thin-walled beam. Symmetrical notches in four corners cause the structure to cripple along the beam axis and prevent from overall bending.

For the fourth model, a bumper beam is added to a notched direct beam. These changes should be in a way to prevent the overall bending and cause plastic deformation in the longitudinal axis of the direct beam and collapsing of the bumper happens in advance. Crippling and the impact time of the accident will also be increased.

A 0.35 m long beam with a 75 mm square cross section was used, along with two symmetrical notches in four corners of the cross section according to Alavi Nia et al. results. The place of notches was selected near the bumper beam to collapse along with it. The selected St52 steel direct beam has 2 mm in thickness. The scheme of the fourth model is seen in Fig. 4. The bumper beam has a thickness of 2 mm in the fourth model.

Fifth Model

The fifth model is similar to the fourth model except for the thickness of the bumper beam which is 1 mm.

In all of the models, plates with 5 mm thickness and 0.1 m square section are used to connect these beams. The materials of these plates are similar to the material of the beams that they are connected to by welding. One of the plates between the direct and the bumper beams is made of St52 steel and the other is Al6063 aluminum alloy, and they are connected to each other by bolts.

The United States of America standard of FMVSS No. 208 and the Economic Commission for Europe standard of ECE No. 94 were used to study the safety in a frontal crash. FMVSS No. 208 standard consists of two tests with velocities of 15.55 and 11.11 m/s, with rigid barrier by complete overlap and angular

rigid barrier, respectively. ECE No. 94 standard consists of one test with a velocity of 17.77 m/s and an offset deformable barrier [17, 18].

2. Performance indicators Specific energy absorption

Specific energy absorption index is used to compare the energy absorption of beams of chassis front rails for each suggested model. The specific energy absorption index is obtained from division of the absorbed energy or the area under the load-displacement curve by the mass of the structure as shown in the Eq. (1).

$$SAE = \frac{E_{Absorb}}{M} = \frac{\int P d\delta}{M}$$

In which, P is the total inserted load on structure, δ is plastic deformation, and M is structure mass.

Injuries to head

One of examining indexes for physical injuries in front accident is injuries to occupants or Head Injury Criteria (HIC 15). This index is obtained from Eq. (2).

$$HIC = \left[\frac{1}{t_1 - t_2}\int_{t_1}^{t_2} a_r dt\right]^{2.5}(t_2 - t_1)$$

In which, dt is 0.015 s and a_r is obtained from Eq. (3).

$$a_r = \sqrt{a_x^2 + a_y^2 + a_z^2}$$

In which, ax , ay and az shows the input acceleration on passenger head in the three main directions [17, 18].

The criterion of input injuries to the head of occupants is dependent on time according to relations (2) and (3). More increase in vehicle crash time leads to less acceleration and injuries to passenger's head. Since air bag of the vehicle reaches to its maximum volume and load in 0.04 s, vehicle crash time must be more than 0.04 s for dummy head to hit air bag before the end of crash time and reduce the injuries to occupants. The ideal value of HIC 15 is 700. Insurance Institute for Highway Safety ranks head injuries according to Table 1 [19].

Table 1.Ranking the injuries to head [19].

HIC 15			
Good	Acceptable	Marginal	Poor
< 560	560 – 700	700 – 840	840 <

Table 1 Ranking the injuries to head [19].

HIC 15			
Good	Acceptable	Marginal	Poor
< 560	560 – 700	700 – 840	840 <

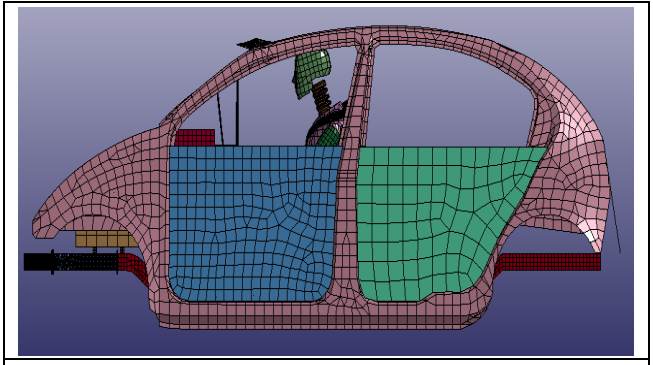

Fig. 5. Elemental model of vehicle.

3. Modelling with Finite Elements

The explicit finite element method of LS DYNA software was used to examine the simulation and numerical solution.

3D Solid elements were used for elements of the plates at the end of the beams. The Shell elements are selected for vehicle body elements, main chassis and chassis beams due to large length to thickness ratio and 6 degrees of freedom. In order to reduce calculation volume and solution time, the Belytscko-Tsay formula is used to formulate Shell elements which use reduced integration with one integration node in the center of an element [20]. To increase calculation accuracy, three to nine integration nodes along the thickness are selected based on the imposed load on the member and its plastic deformation. Nine nodes of integration are selected for direct and bumper beams and five nodes along the thickness are chosen for curved beam and main chassis.

Elements with various dimensions are used depending on its location and its importance in loading. Smaller dimensions are used to increase solution accuracy for the bumper beam, direct beam, air bag, and dummy due to the high role of these elements in crash and loading.

The material of the bumper beam is Al6063 aluminum alloy and for the other members is St52 steel. The Johnson-Cook model is implemented for modelling of members' material because of its ability to model the possible failure of the members during the loading. The stress relation in Jonson-Cook model is as Eq. (4).

$$\sigma = \left[A + B\varepsilon^{n}\right]\left[1 + C\mathrm{Ln}\dot{\varepsilon}^{*}\right]\left[1 - T^{*m}\right] \quad (4)$$

In Eq. (4), σ is stress of Johnson-Cook, ε is plastic strain of Johnson-Cook, $\dot{\varepsilon}^{*} = \dot{\varepsilon} / \dot{\varepsilon}0$ is plastic strain rate, T*= (T - TRoom) / (TMelt - TRoom) and $\dot{\varepsilon}0$ = s-1. A, B, C, m and n are constants obtained by the experiments on the selected material and is unique for each material. Failure strain is also obtained from Eq. (5) for Johnson-Cook model.

$$\bar{\varepsilon}_{f} = \left[D_1 + D_2 \exp(D_3 \eta)\right]\left[1 + D_4 \mathrm{Ln}\dot{\varepsilon}^{*}\right]\left[1 + D_5 T^{*}\right] \quad (5)$$

In this Equation, $\bar{\varepsilon}f$ is failure strain of Johnson-Cook. The ratio of stress to strain is defined by η = σm / σ in which σm is the average of three main stresses and D1 – D5 are obtained constants from the experiment on the mentioned material and are unique for each material [20]. The results of the tests for obtaining the constants of these two materials are presented in references [21] and [22].

Single Surface contact model is defined for the structure contact to itself and crippling of the direct beam, the bumper beam, and the body. To obtain more accurate solution, both Surface to Surface and Node to Surface contacts types are used in loading and contact for important members such as the bumper beam contact to the barrier and the dummy crash to the air bag [23].

Dummy model is available in the software. SAE J1100 standard was used for putting and modeling all body element's angles inside the vehicle in comparison to each other [24]. As for the safety belt, the mounting points and the midpoints along with the areas contacting the members were modeled.

Considering the minor impact of the car suspension and moving systems on the results and in order to reduce the solution time, modeling of these members were ignored. Fig. 5 demonstrates the elemental model of the vehicle.

5. Results and Discussion Plastic Deformation

Figs. 6-10 shows the plastic deformation during vehicle accident for the five suggested models. The results show that the bumper beam in model 2, 3 and 5 is totally crippled, and its deformation is not in form of overall bending due to its shorter length and its lower resistant material. It also collapsed sooner than the direct beam during the crash. The bumper beam was not crippled in the fourth model due to its high resistance in comparison to the direct beam.

In models 1, 2, and 3, it is shown that the direct beam had overall bending due it's high length and hardness and no crippling is observed. Overall bending of the direct beam in these 3 models made high deformation in the curved beam and damaged the main chassis. Moreover, overall bending in the direct beam made the vehicle front components enter the occupants' cabinet and probably hurting them. As the bumper beam was thicker in model 4 than model 5, it had less plastic deformation and energy absorption and transferred energy to the main chassis and this again caused the vehicle front components to enter the occupants' cabinet and probably hurting them. It was observed in results of models 4 and 5 that using the symmetrical double-head notches in the direct beam cross section started the crippling form the notched section. Using the notches made the direct beam collapse in longitude axis of the direct beam and reduced the imposed damages on the curved beam and the main chassis.

According to the above results, it is observed that the objective of the model 5 which was having more plastic deformation and crippling in longitude axis of the bumper beam

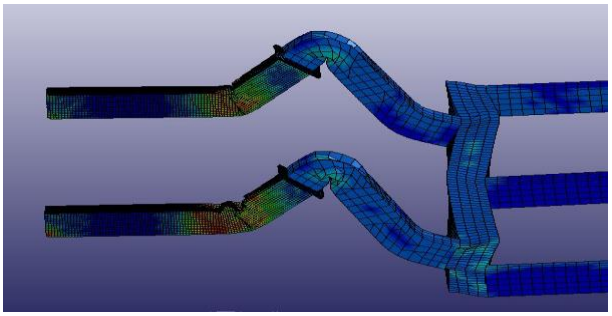

Fig. 6. The first model plastic deformation.

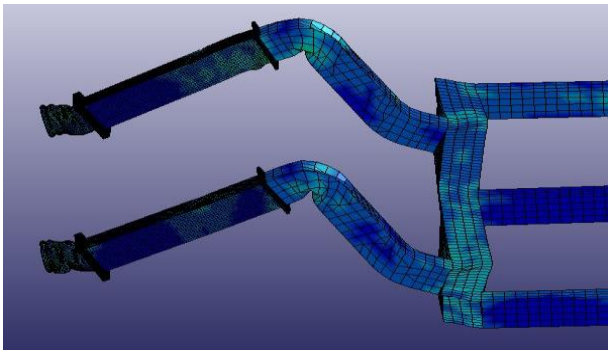

Fig. 7. The second model plastic deformation.

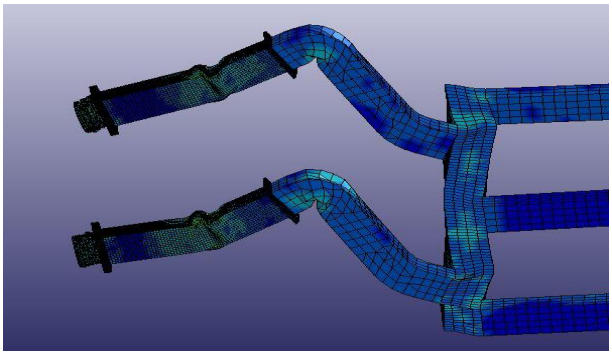

Fig. 8. The third model plastic deformation.

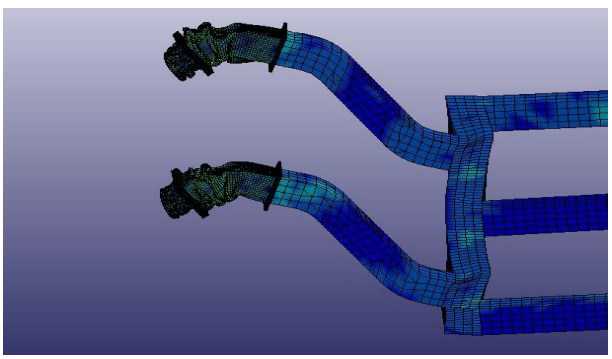

Fig. 10. The fifth model plastic deformation.

4. Displacement of the Curved Beam

The relative displacement of the curved beam in the main coordinate X is shown in Fig. 11. X axis is parallel to the length of the vehicle. The relative displacement is measured with respect to the center of chassis. It is observed in Fig. 11 that the fifth model has the minimum movement and plastic deformation. In other words, the curved beam and main chassis in the fifth model have the minimum deformation and penetration to occupants' cabinet.

5. Energy Absorption

The design objective was for the direct and bumper beams to have maximum energy absorption and the main chassis and the curved beam to have minimum plastic deformation and energy absorption. Table 2 demonstrates that the bumper beam added to models 2 to 5 absorbs a part of the energy and then the transfer of energy to other members is reduced. Since this beam had the maximum energy absorption for model 4 and 5 than models 2 to 3 during plastic deformation and crippling, the transferred damage and energy to the main chassis is reduced. It is observed that the bumper beam had less plastic deformation for more thickness in model 4 than model 5.

It is shown in Table 3 that the specific energy absorption in model 4 and 5 had a significant increase in comparison to that of models 2 and 3 with relatively similar dimensions. This indicates that the increase in specific energy absorption is due to more energy absorption and plastic deformation resulted from notches in model 4 and 5. Specific energy absorption for the main chassis reduced because of less plastic deformation in models 4 and 5 in comparison with three other models. This indicates the transfer of energy absorption from the main chassis and cabin to the permitted area of front chassis rails. As observed in model 4, the bumper beam had less energy absorption and plastic deformation than model 5. Thus, according to specific energy absorption, plastic deformation of the fifth model is the most proper.

Crash Time

The time duration of the vehicle crashing into the barrier is shown for suggested models in Fig. 12. It is observed in Fig. 12 that the crash time increased for models 4 and 5 because longitudinal notches are used in the direct beam. The increase in crash time indicates an increase in plastic deformation of vehicle members and a decrease in the imposed acceleration on the vehicle. According to Fig. 12 models 4 and 5 had tangible crash time increase of 29% and 34% respectively in comparison to other three models due to crippling of direct beam resulting more plastic deformation.

6. Injuries to Occupants' Body

The imposed injuries on head depend on the head acceleration and the crash time of the vehicle. Since the air bag reaches to its maximum load and volume in 40 ms, fewer injuries would be imposed to occupants if the crash time becomes more than 40 ms. It is observed in Table 4 that models 4 and 5 have the lowest amount of occupant's injuries due to the increase in plastic deformation and crash duration. Since in the fourth model, the bumper beam resistance is more than the curved and direct beam resistance, crash energy is transferred to the curved beam and the curved beam has more plastic deformation which causes the vehicle front components enter the occupants' cabinet and probably hurt the occupants' legs. Generally, the model 5 is the safest model for the vehicle chassis having the lowest imposed injuries to occupant's body.

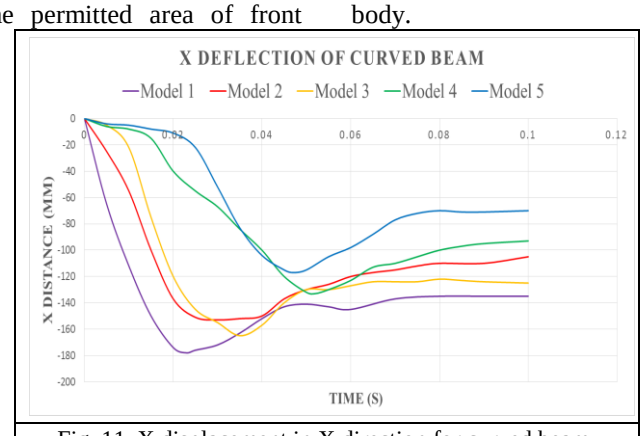

Fig. 11. X displacement in X direction for curved beam.

Table 2
The absorbed energy by chassis members

Energy Absorption (kJ)	Bumper Beam	Direct Beam	Main chassis
The first model	0	15	32
The second model	20	2	24
The third model	12.5	7	25
The fourth model	4	28	8
The fifth model	10	23	9

Table 3
Specific energy absorption by chassis members.

SEA (KJ/kg)	Bumper Beam	Direct Beam	Main chassis
The first model	0	3.333	0.328
The second model	21.95	0.634	0.246
The third model	27.17	2.222	0.256
The fourth model	4.395	9.459	0.082
The fifth model	21.30	7.777	0.092

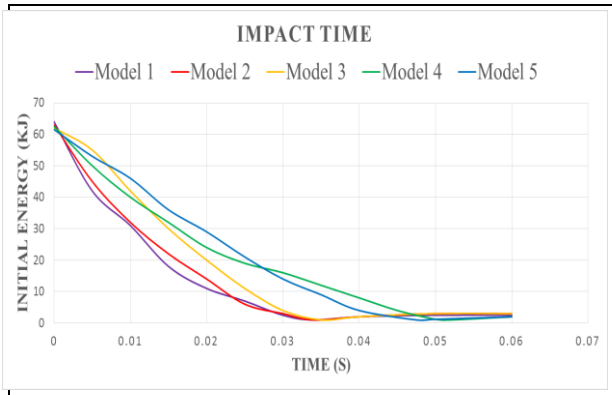

Fig. 12. Crash time for suggested chassis models of vehicle.

7. Final model for chassis front rail of vehicle

By investigating the results of impact for suggested models, it is observed the fifth model is the most suitable model for chassis front rails of the vehicle. By selecting the fifth model for chassis front rails of the vehicle, crash simulations for two tests of FMVSS No. 208 standard and single test of ECE No. 94 standard were performed. Results for occupants head injuries and crash time are presented in Table 5. It is observed in all three tests that crash times were more than 40 ms. Also, it is observed that injuries of occupants are in the allowed range for all three tests and no serious injury is observed.

Table 4
Imposed injuries on suggested models chassis of vehicle.

Head Injury Criteria 15		Good <560	Acceptable 560-700	Marginal 700-840	Poor 840<
The first model	Drive				5331
	Passenger				4806
The second model	Driver				4480
	Passenger				2763
The third model	Driver				4307
	Passenger				3529
The forth model	Driver	509			
	Passenger	495			
The fifth model	Driver			767	
	Passenger		632		

Table 5
Head injuries and crash time on final chassis of vehicle.

Barrier	Safe Belts	Velocity (m/s)	Crash Time (ms)	Occupants	Good <560	Acceptable 560-700	Marginal 700-840	Poor 840<
Angular Rigid	No	11.11	75	Driver	150			
				Passenger	204			
Full Rigid	Yes	15.55	47.5	Driver			767	
				Passenger		632		
Offset Deformable	Yes	17.77	67.5	Driver		571		
				Passenger				927

6. Conclusion

In this article, the vehicle-barrier crash was studied for 5 suggested models of chassis front rails with the purpose of selecting the proper model. The objective of this study was examining the plastic deformation and more energy absorption by the chassis front rails of the vehicle and increasing vehicle crash time for the higher safety of vehicle occupants. The results showed that in models 2 to 5 the added bumper beam increased the crash energy absorption and transferred the crash energy to the bumper beam in which reduced the imposed load to the main chassis and the occupants' cabin.

The results of models 4 and 5 demonstrate that making a symmetrical double-head notch in the direct beam caused crippling, plastic deformation, and more energy absorption in the direct beam. This would increase the vehicle-barrier crash time to about 29% and 34% in comparison to the other three models and reduce the imposed injuries to the vehicle occupants. The results of imposed injuries to the head of the occupants properly show the effect of the vehicle crash time on head injuries. Occupants' legs were injured due to the entrance of the vehicle front components to the occupants' cabinet in models 1 to 4. Moreover, the minimum deformation of the curved beam in the fifth model indicates the minimum penetration to the occupants' cabinet and thus more safety.

After selecting the fifth model for chassis front rails of the vehicle, simulations of crash tests of selected model for two tests of FMVSS No. 208 standard and single test of ECE No .94 standard were performed. From results of passengers' injuries and crashes time, it is observed that the selected model is an appropriate model for chassis front rails of the vehicle.

Generally, adding the bumper beam and optimizing the direct beam design and transferring the energy absorption from the main chassis and the occupants' cabinet to the permitted area of front chassis rails, increases vehicle crash time and occupants' safety. In addition, the bumper beam, the direct beam, and the curved beam resistance must be selected so that it would lead to collapse and crippling of the bumper beam, the direct beam, and the curved beam, respectively.

7. References

[1]. Mohamed Sheriff N, Gupta NK, Velmurugan R, Shanmugapriyan N. Optimization of thin conical frusta for impact energy absorption. Thin-Walled Structures 2008; 46: 653–66.

[2]. Zhang C, Saigal A. Crash behavior of a 3D S-shape space frame structure. Journal of Materials Processing Technology 2007; 191: 256–9.

[3]. Oliveira D, Worswick M, Grantab R, Williams B, Mayer R. Effect of forming process variables on the crashworthiness of aluminum alloy tubes. International Journal of Impact Engineering 2006; 32: 826–46.

[4]. Tang Z, Liu S, Zhang Z. Analysis of energy absorption characteristics of cylindrical multi-cell columns. Thin Walled Structures 2013; 62: 75–84.

[5]. Yang S, Qi C. Multiobjective optimization for empty and foam-filled square columns under oblique impact loading. International Journal of Impact Engineering 2013; 54: 177–91.

[6]. Tarlochan F, Samer F, Hamouda AMS, Khalid K, Ramesh S. Design of thin wall structures for energy absorption applications: enhancement of crashworthiness due to axial and oblique impact forces. Thin-Walled Structures 2013; 71: 7–17.

[7]. Zhang XW, Su H, Yu TX. Energy absorption of an axially crushed square tube with a buckling initiator. International Journal of Impact Engineering 2009; 36: 402–17.

[8]. Zhang XW, Tian QD, Yu TX. Axial crushing of circular tubes with buckling initiators. Thin-Walled Structures 2009; 47: 788–97.

[9]. Cho Yong-Bum, Bae Chul-Ho, Suh Myung-Won, Sin Hyo-Chol. A vehicle front frame crash design optimization using hole-type and dent-type crush initiator. Thin Walled Structures 2006; 44: 415–28.

[10]. Gupta NK, Gupta SK. Effect of annealing, size and cut-out on axial collapse behavior of circular tubes. International Journal of Mechanical Science 1993; 35: 597–613.

[11]. Ohkami Y, Takada K, Motomura K, Shimamura M, Tomizawa H, Usuda M. Collapse of thin-walled curved beam with closed-hat section. Part 1: study on collapse characteristics. SAE Technical Paper 900460; 1990.

[12]. Nishigaki K, Ishivama S, Ohta M, Takagi M, Matsukawa F, et al. Collapse of thin-walled curved beam with closed-hat section. Part 2: Simulation by plane plastic hinge model. SAE Technical Paper 900461; 1990.

[13]. Zhou Y, Lan F, and Chen J. Crashworthiness research on S-shaped front rails made of steel–aluminum hybrid materials. Thin-Walled Structures 2011; 49: 291-97.

[14]. Tanlak N, and Sonmez O. Optimal shape design of thin-walled tubes under high-velocity axial impact loads. Thin-Walled Structures 2014; 84: 302-12.

[15]. Dass Goel M. Deformation, energy absorption and crushing behavior of single-, double- and multi-wall foam filled square and circular tubes. Thin-Walled Structures 2015; 90: 1-11.

[16]. AlaviNi YA, FallahNejad Kh, Badnava H and Farhoudi HR. Effects of buckling initiators on mechanical behavior of thin-walled square tubes subjected to oblique loading. Thin-Walled Structures 2012; 59: 87-96.

[17]. Federal Motor Vehicle Safety Standards No. 208. Occupant Crash Protection. National Highway Traffic Safety Administration. 49 CFR Parts 552, 571, 585 and 595.

[18]. Economic Commission for Europe Regulation No. 94, Protection of the Occupants in The Event of a Frontal Collision, 2003.

[19]. Small Overlap Frontal Crashworthiness Evaluation Rating Protocol. Insurance Institute for Highway Safety. 2014.

[20]. LS-DYNA Manual Volume 2. Material Models. August 2012.

[21]. Wang k. Calibration of the Johnson-Cook Failure Parameters as the Chip Separation Criterion in the Modelling of the Orthogonal Metal Cutting Process. McMaster University. 2016.

[22]. Seidt D, Gilat A and Klein A. High Strain Rate, High Temperature Consititutive and Failure Models for EOD Impact Scenarios 2007. SEM-Ann-Conf-s05p01.

[23]. LS-DYNA Manual Volume 1. August 2012.

[24]. SAE J1100. Motor Vehicle Dimensions. Society of Automotive Engineers. 1984.